Light Metals 2012 *Edited by: Carlos E. Suarez*
TMS (The Minerals, Metals & Materials Society), 2012

Light Metals 2012

ALUMINUM ALLOYS: Fabrication, Characterization and Applications

Emerging Technologies

SESSION CHAIR
Subodh Das
Phinix, LLC
Lexington, Kentucky, USA

Light Metals 2012 *Edited by: Carlos E. Suarez*
TMS (The Minerals, Metals & Materials Society), 2012

Effect of tool rotational speed on the microstructures and tensile properties of 7075 aluminum alloy via Friction Stir Process (FSP)

Ming-Hsiang Ku*[1], Fei-Yi Hung[2], Truan-Sheng Lui[1] and Li-Hui Chen[1]
[1] Department of Maerials Science and Engineering, National Cheng Kung University, Tainan, TAIWAN 701
[2] Institute of Nanotechnology and Microsystems Engineering, Center for Micro/Nano Science and Technology, National Cheng Kung University, Tainan, TAIWAN 701
*Email:n58961016@mail.ncku.edu.tw

Abstract

7075-T6 aluminum alloy plates were subject to FSP with various tool rotational speeds (1230, 1450 and 1670 rpm) followed by different heat treatments (natural aging and T4T6 treatments). The influences of tool rotational speeds and aging treatments on the microstructures and tensile properties were discussed. The experimental results showed that the tensile strength of FSPed specimens with various tool rotational speeds were close. After aging treatments, higher tool rotational speeds (1670 rpm) had an embrittlement phenomenon on the SZ due to the contribution of low element bands (LEBs) and precipitates. EPMA analysis showed that the LEBs are low element distributions, such as Zn, Mg, Cu. Decreasing the tool rotational speeds, the LEBs were not obvious and restrained the brittle behavior to improve the ductility. Compared with natural aging, after T4T6 treatments, the tensile strength of FSP specimens with all tool rotational speeds was improved obviously.

Keywords: friction stir process, tool rotation speeds, low element bands

1. Introduction

7xxx series aluminum alloys are the heat treatment alloys which produce precipitates (such as $MgZn_2$) to raise the mechanical strength. 7075 (Al-Zn-Mg-Cu) aluminum alloy is widely applied as large structural components in aerospace navigation and transportation facilities, due to their good combination of strength, hardness and fracture toughness.[1-3] However, 7075 aluminum alloy is difficult to join by traditional welding due to the defects (such as voids and dendritic structures) in the fusion zone. Friction stir welding (FSW) is a good method to avoid the defects of traditional welding.

FSW/FSP[4-5] is a solid-state technique where the temperature of friction stir welding/process had not reached the melting point. Hence, there were not many porosities and shrinkage cracks inside the material. The specimen can produce fine recrystallized grains in the stir zone due to the severe plastic deformation by rotating of the friction tools. However, the characteristics of plastic deformation is closely related to the mechanical properties, its high energy deformation mechanism has still not been examined, and in particular the brittle behavior.[6-9]

M. Mahoney and co-workers indicated that the embrittlement phenomenon of 7075 aluminum alloy occurred in the SZ by FSW and artificial aging (121℃ , 24h).[10] It has been said that the precipitate distribution and precipitate-free zone (PFZ) were the main reason, but that is not strictly true. It must be noted that the relation among the distribution of elements, deformation degree and LEBs has not yet been investigated. Notably, the effects of the LEBs and fine equiaxed grains in the SZ how to induce embrittlement behavior of SZ for 7075 aluminum alloy through aging treatments is an important role in the applications. In this study, the density of LEBs in the SZ of 7075 aluminum alloy was different under the various tool rotational speeds of FSP, and then the effect of FSP through aging treatments (natural aging, NA and T4T6 treatments) on microstructure and mechanical properties of 7075 aluminum alloy with FSP was investigated to clarify the embrittlement mechanism of tensile fracture of the fine equiaxed microstructure.

2. Experimental Procedure

The material used in this study was a 5mm-thick 7075 Al-Zn rolled plate. The specimen had the solution treatment and T4T6 heat treatment to obtain 7075-T6 aluminum alloy as a base metal. The chemical composition (in wt%) was Al-5.7Zn-2.4Mg-1.7Cu-0.3Cr-0.2Fe. The processing direction of the FSP was parallel to the rolling direction. Three tool rotational speeds were performed as 1230, 1450 and 1670 rpm; tool moving speeds were fixed at 0.58 mms^{-1} with 1.5° of tool angle; the downward push force was controlled at the 39 MPa. After FSP, the specimen were performed with two aging treatments : natural aging (40℃, 96h)

and T4T6 treatments. The base metal of specimen would be designated as "BM", and the 1230 rpm FSPed specimen (un-natural aging, as-FSPed) and then via two aging treatments (NA and T4T6 treatments) would be designated as "1230R as-FSPed", 1230R-NA and 1230R-T4T6, respectively. The other tool rotational speeds of FSPed specimens were designated likewise.

While the temperature of the friction center reached solution temperature during FSP, the SZ produced a part of solution phenomenon and occurred natural aging. In order to understand the aging behavior after FSP, the FSPed specimens were performed two aging treatments and investigated the microstructures and mechanical properties at various tool rotational speeds. The characteristics of microstructure at every tool rotational speeds after FSP were analyzed, and then the variation of the grain size will be calculated and the Vickers-Hardness was tested with a load 0.49N for 10s to understand the distribution of relation with the LEBs and the micro-hardness in the experiment.

In addition, the tensile properties of FSPed specimens were performed before (as-FSPed) and after aging treatments (NA and T4T6 treatments). The direction of tensile specimen was parallel to the rolling direction (friction stir direction) and the gauge length contained the SZ. The strain rate was fixed at 1.67×10^{-3} s^{-1}. The different deformation degrees of SZ always varied with friction stir rotational speed to affect the precipitate distribution and the uniformity of structure. The distribution morphology of elements and the LEBs were analyzed by EPMA and nanoindenter to clarify the tensile embrittlement of FSPed specimens.

3. Results and Discussion

3.1 Microstructures

The microstructure of BM was a Pancake Structure along RD (rolling direction) and TD (transverse direction), as shown in Fig. 1. Figure 2 show the microstructure of PD plane in the friction zone. According to the plastic deformation degree and heat-input in the friction stir zones, it can be distinguished stir zone (SZ), thermomechanically affected zone (TMAZ) and heat-affected zone (HAZ).

The deformation degree of the SZ varied with the stir rotational speed increasing. Comparing with three tool rotational speeds (1230, 1450 and 1670 rpm) structures, there was an obvious refinement in the equixaed grains of SZ, as shown in Fig. 3. The average grain sizes were 5.2, 5.1, 4.2 μm from low to high tool rotational speeds. In addition, the average grain sizes of three FSPed specimens were slightly coarse (6.0, 6.1, 5.9 μm) after T4T6 treatments(Fig. 4).

3.2 Mechanical properties

In the experiment, advancing side (AS) is defined as the direction of tool rotation with the same direction as processing direction; retreating side (RS) is defined as the direction of tool rotation with the reverse direction of processing direction. Figure 4 shows the hardness of PD plane (the test location was approximately 1mm under the upper surface), the results revealed that the micro-hardness of three FSPed specimens via natural aging or T4T6 treatments were higher than that of as-FSPed specimen. The micro-hardness of three FSPed specimens via natural aging were lower than that of BM specimen, but the micro-hardness of three FSPed specimens via T4T6 treatment were higher than that of BM specimen.

Figure 5 shows the tensile properties of as-FSPed specimens and aging treatment (NA and T4T6 treatments) specimens. The results revealed that the YS and UTS of as-FSPed and natural aging specimens were lower than those of BM specimen. In addition, The FSPed specimens via natural aging had different YS and UTS. The YS and UTS of 1230R-NA and 1450R-NA specimens slightly increased, but those of 1670R-NA specimens slightly decreased. However, the YS and UTS of 1230R-T4T6, 1450R-T4T6 and 1670R-T4T6 specimens were nearly the same as those of BM specimens. To estimate the embrittlement of FSPed specimens by elongation, it was found that the UE and TE of FSPed specimens were lower than those of BM specimen. Regardless of the FSPed specimens via natural aging or T4T6 treatments, the UE and TE of 1230 rpm specimens were obviously promoted, and those of 1670 rpm specimens were deteriorated. Remarkably, the UE and TE of 1450 rpm specimens appeared a great variation. In other words, increasing the tool rotational speeds resulted in an embrittlement behavior in the SZ, this even was more obvious after aging treatments.

3.3 Embrittlement mechanism

For the high tool rotational speed condition, the aging treatments (NA and T4T6 treatments) certainly affected the embrittlement mechanism (the low deformation degree was not obvious) from the datas of 1670R as-FSP, 1670R-NA and 1670R-T4T6 specimen. In other words, the precipitate distribute for aging treatments

and the density of LEBs both affected the embrittlement mechanism in the SZ. The specimen with natural aging was analyzed by EPMA to clarify the relationship between the plastic deformation degree of FSP and the distribution of LEBs. Figure 6 shows that the elements (including Zn, Mg and Cu) of 1230R-NA specimen were uniformly distributed in the SZ, but those of 1670R-NA specimen had less elements in the LEBs. They demonstrate that the high tool rotational speed not only has obvious the LEBs but also results in non-uniform distribution of the elements.

Judging from the above, in order to understand the relationship between the hardness of LEBs and distribution of elements, the hardness of LEBs and the area around were measured using a nanoindenter (Fig.7). Fig. 7(a) shows the 1670R-NA specimen has many LEBs. According to the nano-indention data (Fig 7(b)), the hardness of LEBs was higher than that of non-LEBs in the SZ after natural aging. It is obvious that the deformation resistance of LEBs was different in the SZ. Therefore, during the tensile test, the interface between the LEBs and non-LEBs in the SZ has stress concentration to cause the crack easily. Due to the LEBs and the precipitation hardening, the high tool rotational speed of FSPed specimen had the embrittlement. These are the reasons why the elongation of 1670 rpm specimen had decreased from ~10% to 3%(Fig. 5).

4. Conclusions

After FSP, 7075-T6 Al alloy had fine equiaxed structure and the average grain size decreased with increasing the tool rotation speeds in the stir zone. The tensile strength of all tool rotational speed specimens via T4T6 treatments were nearly the same as those of BM specimen. Higher tool rotational speeds, which caused the LEBs to affect the mechanical properties after aging treatments. The LEBs had higher deformation resistance and non-uniform precipitated hardness that resulted in the embrittlement in high tool rotational speed of FSPed specimens.

Reference

(1) B. Smith: Adv. Mater. Process., 161. No. 9 (2003), 41-44.
(2) B. Kumar, C. Widener, A. Jahn, B. Tweedy, D. Cope and R. Lee: 46th Structural Dynamics & Materials Conference, (2005) pp.1.
(3) W. M. Thomas and E. D. Nicholas: Mater. Des., 18(1997) 269-273.
(4) Z. Y. Ma, R. S. Mishra and M. W. Mahoney: Acta Mater. 50 (2002) 4419-4430.
(5) R. S. Mishra, M. W. Mahoney, S. X. McFadden, N. A. Mara and A. K. Mukherjee: Scripta Mater. 42 (2000) 163-168.
(6) F. J. Humpheys and M. Hathrly: Recrystallization and Related Annealing Phenomena, (Pergamon, Oxford, UK, 1996) pp.363-392.
(7) K. V. Jata and S. L. Semiatin: Scripta Mater. 43 (2000) 743-749.
(8) J. Q. Su, T. W. Nelson, R. Mishra and M. Mahoney: Acta Mater. 51 (2003) 713-729.
(9) C. G. Rhodes, M. W. Mahoney, M. H. Bingel and M. Calabrese: Scripta Mater. 48 (2003) 1451-1455.
(10) M. W. Mahoney, C. G. Rhodes, J. G. Flintoff, R. A. Spurling and W. H. Bingel: Metall. Mater. Trans. A 29A (1998) 1955-1964.

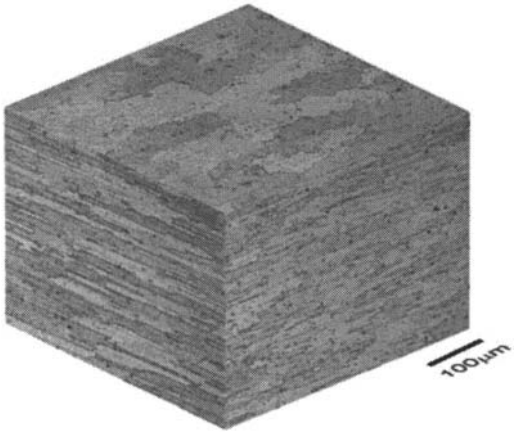

Fig. 1 Optical microstructure of 7075 base metal.

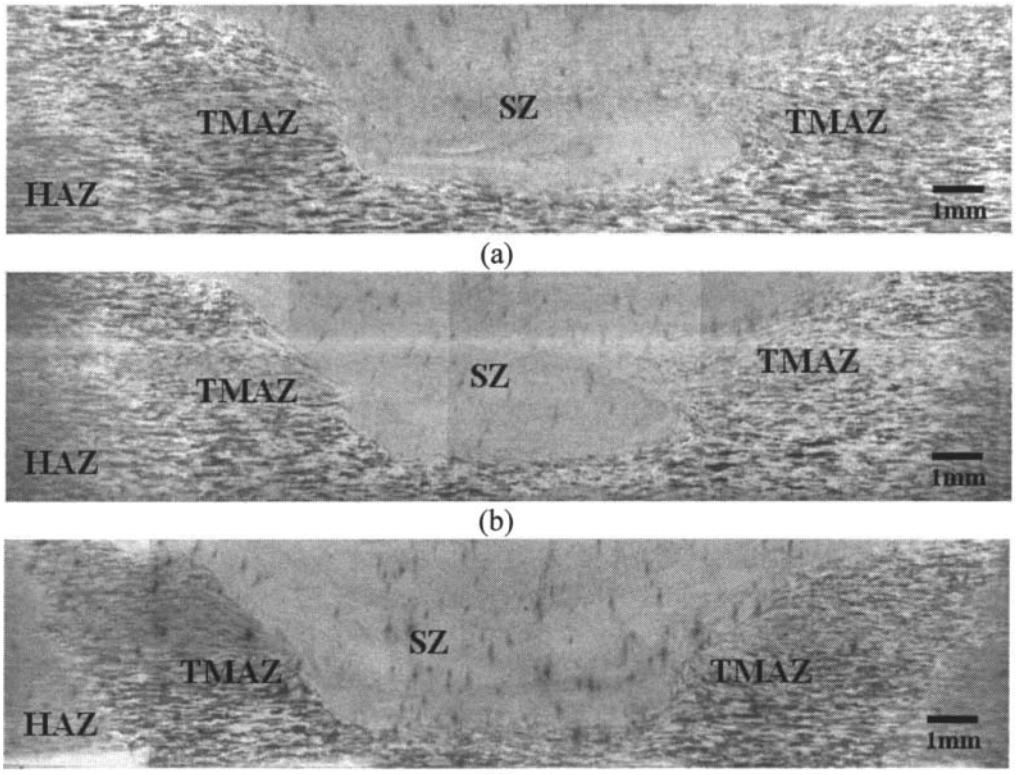

Fig. 2 Cross-section of PD plane for different tool rotational speeds of friction stir process: (a) 1230 rpm, (b) 1450 rpm, (c) 1670 rpm.

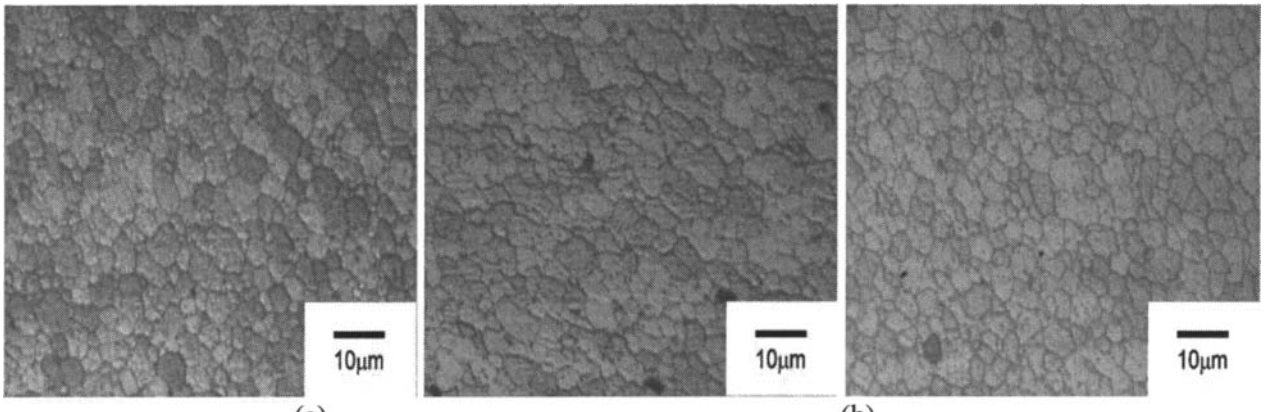

Fig. 3 Microstructures of SZ for different tool rotational speeds:
(a) 1230 rpm, (b) 1450 rpm, (c) 1670 rpm.

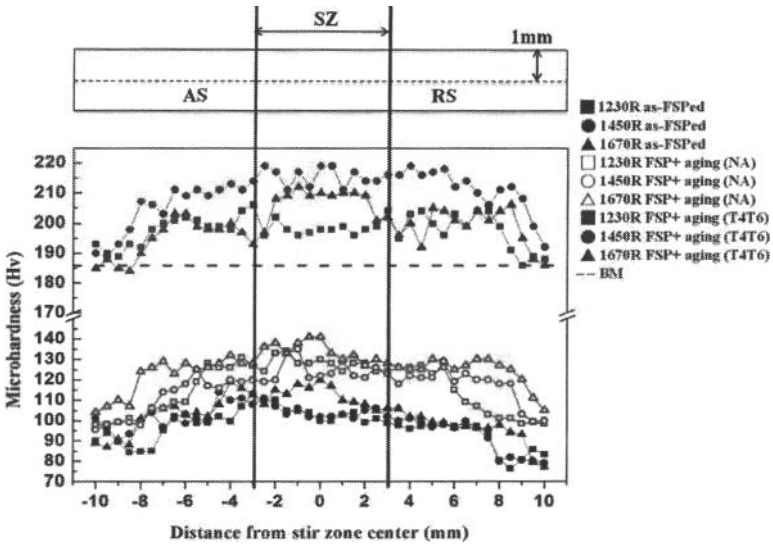

Fig. 4 Micro-hardness profile of PD plane after FSP. The test location was a 1mm under the upper surface.

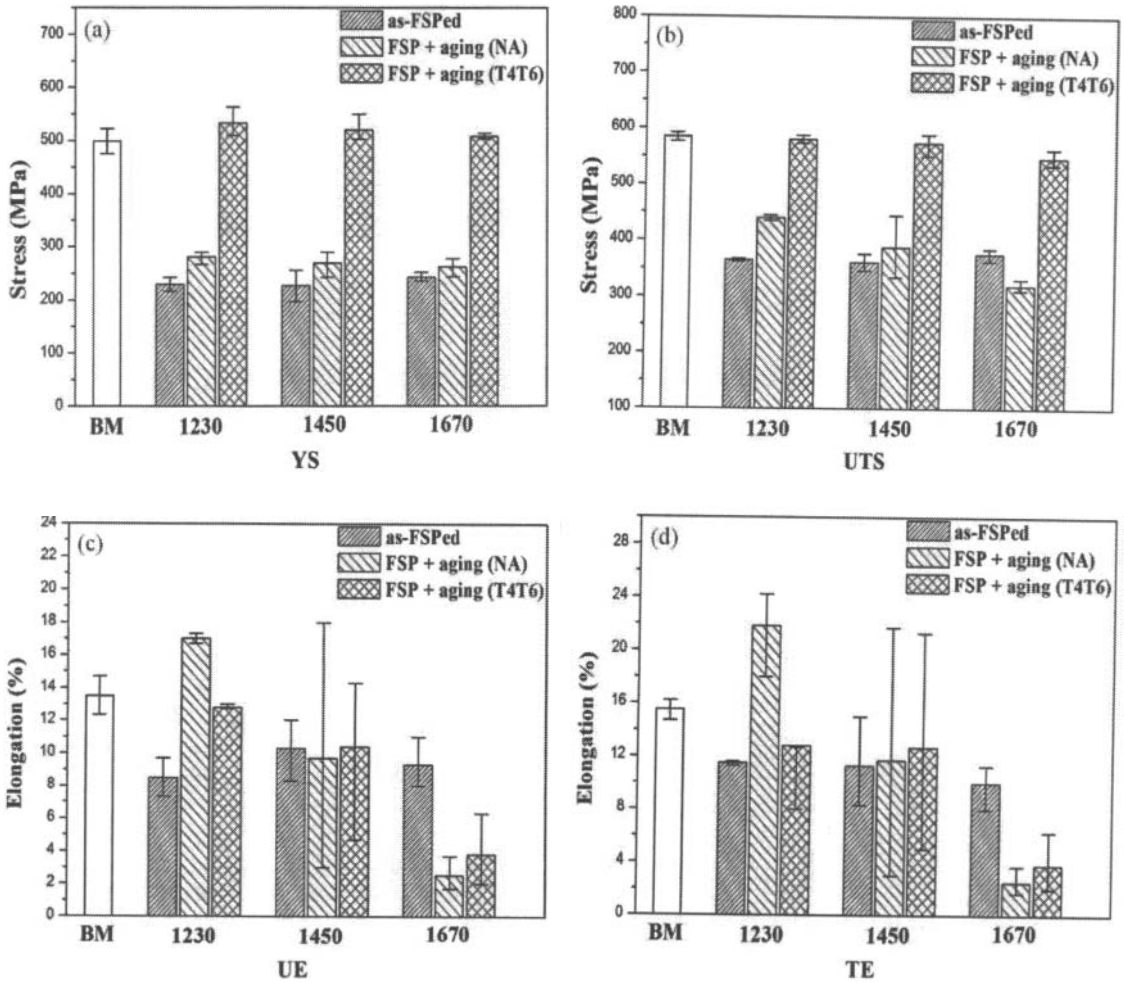

Fig. 5 Tensile properties of as-FSPed specimens and FSP after aging specimens with different tool rotational speeds: (a) YS, (b) UTS, (c) UE, (d) TE.

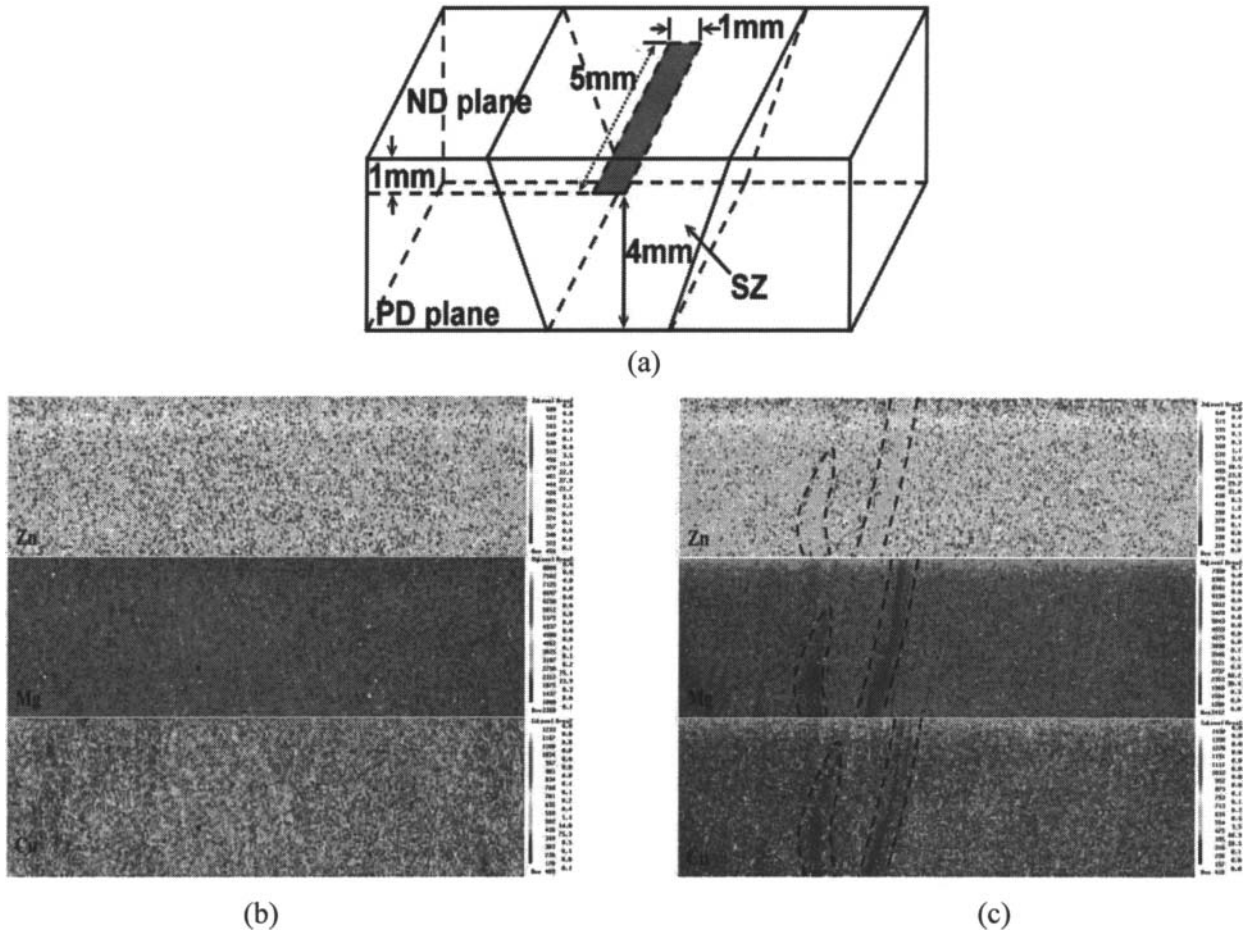

Fig. 6 EPMA of the natural aging specimens with different tool rotational speeds: (a) the location of sample, (b) 1230R-NA, (c)1670R-NA.

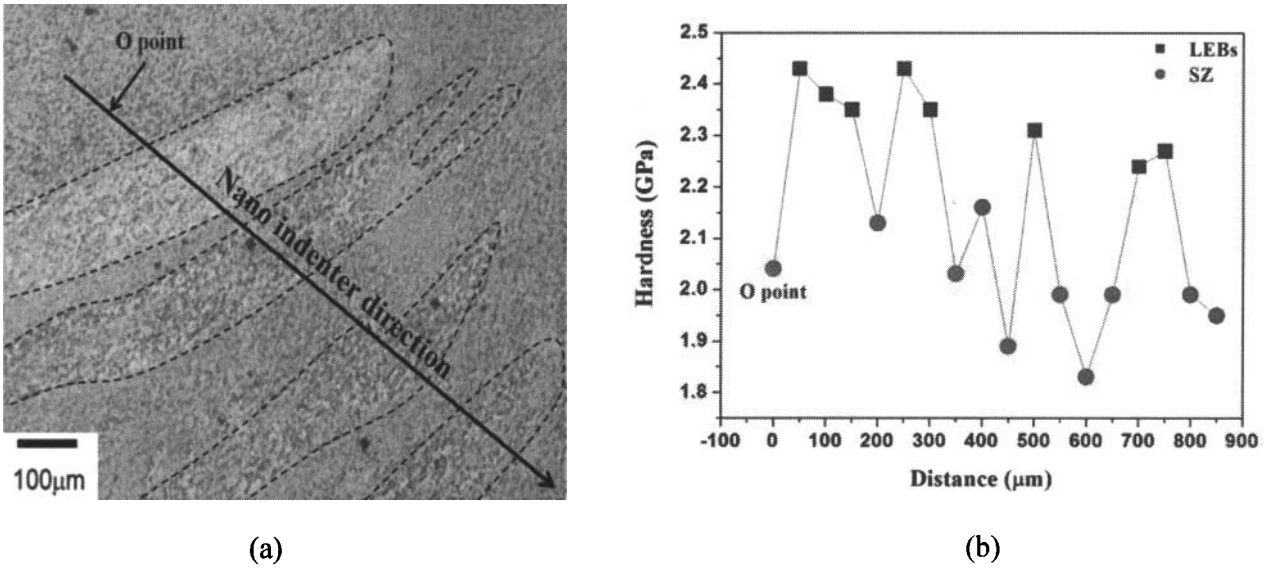

Fig. 7 (a) SZ structure of 1670R-NA specimen, (b) nano indentation hardness of LEBs and the area around.